Year: 2012

Modelling and filtering of physiological oscillations in near-infrared spectroscopy by time-varying Fourier series

Trajkovic, Ivo ; Reller, C ; Wolf, Martin

Abstract: Raw near-infrared spectroscopy signals contain oscillatory components, namely low frequency oscillations (Mayer waves), breathing and the heartbeat. We propose an approach to model and estimate them from noisy measurements assuming that they are linearly superposed. Estimating them is important, since they pose disturbing effects, but they are also of scientific interest. These components are not strictly periodic; we characterize them as "almost periodic." The model of an almost periodic signal is a Fourier series where the Fourier coefficients and the fundamental frequency are allowed to (slowly) change over time. This model can be represented by factor graphs which we use to derive message passing algorithms to estimate the time-dependent model parameters from a measured signal. An implementation of the proposed algorithm processes a 100 s long measurement in 2 s (on a modern PC) which is 10× faster than a comparable previous implementation. Thus, real-time applications, for example, online monitoring, could be realized using slower, inexpensive or power-saving hardware. The increase in speed was achieved by using a different parameterisation of the model which allows Gaussian message passing (with only two parameters: mean and variance), whereas previously some messages were digitized. In the previous implementation, the number of harmonics in the model is chosen manually (for each subject and data channel). In this chapter, we show an intuitive procedure to estimate this number from the measured signal. In conclusion, the proposed algorithm is able to separate the heartbeat and, in contrast to the previous implementation, the low frequency oscillation effectively and in real time.

DOI: https://doi.org/10.1007/978-1-4614-1566-4_45

Originally published at:
Trajkovic, Ivo; Reller, C; Wolf, Martin (2012). Modelling and filtering of physiological oscillations in near-infrared spectroscopy by time-varying Fourier series. In: Wolf, Martin. Oxygen Transport to Tissue XXXIII. New York, NY: Springer, 307-313.
DOI: https://doi.org/10.1007/978-1-4614-1566-4_45

Modelling and Filtering of Physiological Oscillations in Near-Infrared Spectroscopy by Time-Varying Fourier Series

Ivo Trajkovic[a,b], Christoph Reller[c] and Martin Wolf[a,b]

[a]Biomedical Optics Research Laboratory, Division of Neonatology, Department of Obstetrics and Gynecology, University Hospital Zurich, 8091 Zurich, Switzerland
[b]Institute for Biomedical Engineering, University of Zurich and ETH Zurich, 8093 Zurich, Switzerland
[c]Signal and Information Processing Laboratory (ISI), ETH Zurich, 8092 Zurich, Switzerland

Abstract Raw near-infrared spectroscopy signals contain oscillatory components, namely low frequency oscillations (Mayer waves), breathing and the heartbeat. We propose an approach to model and estimate them from noisy measurements assuming that they are linearly superposed. Estimating them is important, since they pose disturbing effects, but they are also of scientific interest.
These components are not strictly periodic; we characterise them as “almost periodic”. The model of an almost periodic signal is a Fourier series where the Fourier coefficients and the fundamental frequency are allowed to (slowly) change over time. This model can be represented by factor graphs which we use to derive message passing algorithms to estimate the time-dependent model parameters from a measured signal.
An implementation of the proposed algorithm processes a 100 s long measurement in 2 s (on a modern PC) which is ~10 times faster than a comparable previous implementation. Thus, real-time applications, e.g. online monitoring, could be realised using slower, inexpensive or power-saving hardware. The increase in speed was achieved by using a different parameterisation of the model which allows Gaussian message passing (with only 2 parameters: mean and variance), whereas previously some messages were digitised.
In the previous implementation, the number of harmonics in the model is chosen manually (for each subject and data channel). In this paper, we show an intuitive procedure to estimate this number from the measured signal.
In conclusion, the proposed algorithm is able to separate the heartbeat and, in contrast to the previous implementation, the low frequency oscillation effectively and in real time.

1 Introduction

We have developed and implemented a method for modelling and adaptive filtering of oscillatory components, in particular the ones caused by (i) the cardiac activity, called “heartbeat”, and (ii) the low frequency oscillations (also Mayer waves), called “LFO”, in signals measured with near-infrared spectroscopy (NIRS), called “raw NIRS signals”. Examples of the latter are the grey curves in Fig. 1A and 1C. The overall aim is to extract each pure signal component, since (i) one disturbs the detection of another, e.g. hemodynamic brain activity and LFO, (ii) then the interrelation between several components can be assessed, and (iii) characterising each component separately could yield new understandings of underlying biological processes.

A traditional band-pass filter [1] will not do, since (i) to include the typical sharp peaks in the heartbeat (grey curve in Fig. 1C), the high cutoff frequency must be rather high; thus, high-frequency noise survives the filtering, (ii) the physiology fluctuates, e.g. the heart rate doubles quickly after starting a physical exercise, and window-based processing allows the harmonics of one or more components, e.g. heartbeat and fast neuronal activity, to spectrally overlap in a window.

Our method has not been tested yet with the breathing component, thus only the heartbeat and the LFO are addressed in this paper.

Strictly periodic signals can be efficiently represented by Fourier series. Let $x_1, x_2, ...$ be the equidistantly sampled version of a strictly periodic real-valued signal, let n be the discrete time index, and let k be the harmonic index. Then

$$x_n = \mathrm{Re}\left(\sum_{k=0}^{\infty} A_k \cdot e^{jkn\Omega} \right) \tag{1}$$

with coefficients $A_0 \in \mathbb{R},\ A_1, A_2, ... \in \mathbb{C}$ and fundamental frequency $\Omega \in [0, 2\pi]$.

We classify the oscillatory components as “almost periodic”, since their period lengths and signal shapes drift over time [2]. We propose to describe such a component by a “Fourier series” with time-variant fundamental frequency (related to the varying period length) and time-variant coefficients (related to the varying signal shape), i.e. we change (1) into

$$x_n = \mathrm{Re}\left(\sum_{k=1}^{K} A_{k,n} \cdot e^{jk\theta_n} \right) \tag{2}$$

with

$$A_{k,n} \approx A_{k,n+1}, \quad \theta_{n+1} = (\theta_n + \Omega_n)_{\mathrm{mod}\, 2\pi}, \tag{3}$$

and

$$\Omega_n \approx \Omega_{n+1}. \tag{4}$$

In this paper, we present an algorithm for estimating the model parameters θ_n which is considerably faster than the algorithm in [2].

When modelling the heartbeat, the magnitude of the coefficients $A_{k,n}$ in (2) typically decays with increasing harmonic index k. Consequently, for $k \geq K$, the harmonics of the heartbeat cannot be distinguished from the noise. The noise energy in raw NIRS signals, and thus K, varies depending on the data channel, NIRS instrumentation and subject; typically $3 \le K \le 7$ whereas $K = 1$ suffices for modelling the LFO. In [2], K was chosen manually (for each subject and data channel); if K is chosen too high, the reconstructed heartbeat will contain noise; if K is chosen too low, high-frequency parts of the heartbeat will not be modelled. At the end of Section 2, we show an intuitive procedure for estimating K from the measured signal.

2 Estimating the model parameters

Let the raw NIRS signal $\mathbf{y} = (y_1, ..., y_N)$ be a noisy, trended version of the signal $\mathbf{x} = (x_1, ..., x_N)$ in (2) where N is the signal length. Specifically,

$$\mathbf{y} = \mathbf{A}_{0,-} + \mathbf{x} + \mathbf{Z} \tag{5}$$

where $\mathbf{Z} = (Z_1, ..., Z_N)$ is discrete time white Gaussian noise, and the trend $\mathbf{A}_{0,-} = (A_{0,1}, ..., A_{0,N})$ models changes slower than the heartbeat, or the LFO respectively, and thus is omitted in (2). We will use the vectors $\mathbf{A}_{k,-} = (A_{k,1}, ..., A_{k,N})$ for $k = 0, ..., K$ and decorate estimates with a hat (e.g. $\hat{\mathbf{C}}$ is an estimate of $\mathbf{C}$).

Given $\mathbf{y}$, the objective is to estimate the phases $\boldsymbol{\theta} = (\theta_1, ..., \theta_N)$, K and the coefficient vectors $\mathbf{A}_{0,-}, ..., \mathbf{A}_{K,-}$ such that $\| \mathbf{y} - \hat{\mathbf{x}} - \hat{\mathbf{A}}_{0,-} \|^2$ is minimal, where $\hat{\mathbf{x}}$ is the reconstructed signal by applying the estimates in (2).

The estimation algorithm consists of several building blocks (see Fig. 2).

Initially, the "A_0 estimator" estimates the slow trend $\mathbf{A}_{0,-}$ by a one-time procedure similar to low pass filtering and based on $\mathbf{y}$ only.

In the heartbeat and the LFO, most of the energy, apart from the noise, lies in the fundamental frequency coefficient $\mathbf{A}_{1,-}$. Thus, a first rough estimate of such an oscillatory component is a complex sinusoid with constant complex magnitude. The "Initial A_1 estimator"-block makes an estimate $\tilde{A}_1$ of this magnitude such that the sinusoid has approximately the same energy as $\mathbf{y} - \hat{\mathbf{A}}_{0,-}$.

The "Phase estimator" calculates the final estimate $\hat{\boldsymbol{\theta}}$ of $\boldsymbol{\theta}$ based on estimates $\hat{\mathbf{A}}_{0,-}$ and $\tilde{A}_1$ and (2) with $K = 1$ parameterised as

$$x_n = \mathrm{Re}\left(\tilde{A}_1 \cdot e^{j\theta_n}\right) = \mathrm{Re}(\tilde{A}_1)\cos(\theta_n) - \mathrm{Im}(\tilde{A}_1)\sin(\theta_n) = \hat{\mathbf{A}}_1 \cdot \mathbf{C}_n \tag{6}$$

with constant vector $\hat{\mathbf{A}}_1 \mathrel{\hat=} \left(\mathrm{Re}(\tilde{A}_1) \quad -\mathrm{Im}(\tilde{A}_1)\right)$. We introduce a state vector $\mathbf{C}_n \mathrel{\hat=} \left(\cos(\theta_n) \quad \sin(\theta_n)\right)^{\mathrm{T}}$ and define a state transition

$$\mathbf{C}_n = \mathrm{rot}(\hat{\Omega}) \cdot \mathbf{C}_{n-1} + \mathbf{U}_n \tag{7}$$

where

$$\mathrm{rot}(\hat{\Omega}) = \begin{pmatrix} \cos(\hat{\Omega}) & -\sin(\hat{\Omega}) \\ \sin(\hat{\Omega}) & \cos(\hat{\Omega}) \end{pmatrix}$$

is a rotation matrix and $\hat{\Omega}$ is a prior estimate of Ω_n in (3). $\hat{\Omega}$ is derived by using the formula in [2], section 3.3, paragraph 4 and assuming a typical heart rate depending on the subject, e.g. $H \mathrel{\hat=} 80$ bpm for adults. Since $\hat{\Omega}$ is fixed, despite the fact that the heart rate varies considerably depending on various factors, uncertainty, i.e. two-dimensional zero-mean white Gaussian noise $\mathbf{U}_\mathrm{n}$ with diagonal covariance matrix $\mathbf{V}$, is added to the rotated state in (7). This addition of noise defines (4). The frequency and its variability (and thus $\hat{\Omega}$ and $\mathbf{V}$) in the LFO are smaller than in the heartbeat.

The estimate $\hat{\mathbf{C}}_n$ of $\mathbf{C}_n$ is made as

$$\hat{\mathbf{C}}_n = \underset{\mathbf{C}_n}{\arg\max}\ f(\mathbf{C}_n \mid \hat{\mathbf{A}}_{0,-}, \tilde{A}_1, \mathbf{y}) \cdot \tag{8}$$

The function f in (8) comprises the equations (5), (6), and (7).

Each estimate $\hat{\theta}_n$ in $\hat{\boldsymbol{\theta}}$ is made as

$$\hat{\theta}_n = \tan^{-1}\left(\frac{\hat{\mathbf{C}}_n(2)}{\hat{\mathbf{C}}_n(1)}\right) \tag{9}$$

with $\hat{\mathbf{C}}_n(i)$ denoting the i-th entry of the vector $\hat{\mathbf{C}}_n$.

In this paper, a node in the factor graph is either (i) the relationship between two or more variables, defined through an equation, or (ii) a prior probability density. Edges are variables.

The “Phase estimator” uses a factor graph containing N consecutive sections one of which is depicted in Fig. 3, i.e the outgoing edge $\mathbf{C}_{n+1}$ of the graph in the figure is at the same time the incoming edge of its right neighbor.

In Fig. 3, the ‘=’-node clones $\mathbf{C}_n$: $\mathbf{C}'_n \triangleq \mathbf{C}_n$ and $\mathbf{C}''_n \triangleq \mathbf{C}_n$; the ‘$\hat{\mathbf{A}}_1$’-node represents (6); the section of the graph with the incoming edge x_n is (5); the section of the graph with the incoming edge $\mathbf{C}''_n$ is (7). The sum-product algorithm for Gaussian messages [3] is applied on the factor graph in Fig. 3 to derive f in (8).

A message (i) is a scaled conditional probability density of the underlying edge, (ii) can traverse the edge in both directions, and (iii) is named μ including an arrow, which indicates the forward ($\vec{\mu}$) or backward ($\overleftarrow{\mu}$) direction with respect to the edge direction, and the name of the underlying edge as a subscript (e.g. $\vec{\mu}_X$).

The schedule of the message passing algorithm on the factor graph in Fig. 3 is:

1. For $n = 1,\ldots,N$, calculate $\overleftarrow{\mu}_{x_n}$ from the measured sample y_n, estimate of the slow trend $\hat{A}_{0,n}$ and the prior probability density $\vec{\mu}_{Z_n}$ represented by the ‘$\mathcal{N}(0,\sigma^2)$’-node.
2. For $n = 1,\ldots,N$, calculate $\overleftarrow{\mu}_{\mathbf{C}'_n}$ from $\overleftarrow{\mu}_{x_n}$ by means of [3], table 3.
3. For $n = 1,\ldots,N$, calculate in sequence (i) $\vec{\mu}_{\mathbf{C}''_n}$ from $\overleftarrow{\mu}_{\mathbf{C}'_n}$ and $\vec{\mu}_{\mathbf{C}_n}$ by means of [3], table 2 ($\vec{\mu}_{\mathbf{C}_1}$ is neutral: $\vec{\mu}_{\mathbf{C}_1} = 1$), (ii) $\vec{\mu}_{\mathring{\mathbf{C}}_n}$ from $\vec{\mu}_{\mathbf{C}''_n}$ by means of [3], table 3, since the rotation of the state $\mathbf{C}_n$ can be expressed as a matrix multiplication (7), (iii) $\vec{\mu}_{\mathbf{C}_{n+1}}$ from $\vec{\mu}_{\mathring{\mathbf{C}}_n}$ ([3], table 2).
4. For $n = N,\ldots,1$, calculate in sequence (i) $\overleftarrow{\mu}_{\mathring{\mathbf{C}}_n}$ from $\overleftarrow{\mu}_{\mathbf{C}_{n+1}}$ ([3], table 2), (ii) $\overleftarrow{\mu}_{\mathbf{C}''_n}$ from $\overleftarrow{\mu}_{\mathring{\mathbf{C}}_n}$ ([3], table 3), and (iii) $\overleftarrow{\mu}_{\mathbf{C}_n}$ from $\overleftarrow{\mu}_{\mathbf{C}''_n}$ and $\overleftarrow{\mu}_{\mathbf{C}'_n}$ ([3], table 2). $\overleftarrow{\mu}_{\mathbf{C}_N}$ is neutral: $\overleftarrow{\mu}_{\mathbf{C}_N} = 1$.
5. For $n = 1,\ldots,N$, calculate the marginal $\tilde{\mu}_{\mathbf{C}_n} = \vec{\mu}_{\mathbf{C}_n} \cdot \overleftarrow{\mu}_{\mathbf{C}_n}$ and then the estimate $\hat{\theta}_n$ according to (8) and (9) with $f \triangleq \tilde{\mu}_{\mathbf{C}_n}$ in (8).

The “Coefficient estimator” uses $\hat{\boldsymbol{\theta}}$ to calculate the full set of coefficient estimates $\hat{\mathbf{A}}_{1,-},\ldots,\hat{\mathbf{A}}_{K,-}$. The used factor graph and message passing algorithms correspond with the ones in [2], section 3.4, with a slight modification.

To derive K in (2), in each iteration step in the “Regularisation”-“Coefficient estimator” loop, the “Regularisation”-block calculates for $1 \leq k \leq K_{\max}$ the noise-to-coefficient ratio $\rho_k \triangleq \| \mathbf{y} - \hat{\mathbf{x}} \|^2 / \| \hat{\mathbf{A}}_{k,-} \|^2$ based on the estimate $\hat{\mathbf{A}}_{k,-}$ and the reconstructed signal $\hat{\mathbf{x}}$ from the previous iteration step. The higher ρ_k, the more the “Coefficient estimator” damps $\hat{\mathbf{A}}_{k,-}$ in the next iteration step. This procedure requires slight modifications in the factor graph of the “Coefficient estimator” which are described in detail in [4]. The estimate of K is the largest $k \in [1, K_{\max}]$ for which $\| \hat{\mathbf{A}}_{k,-} \| > \tau$, where τ is a threshold.

The “Eq. (2)”-block reconstructs the heartbeat, or the LFO respectively, by applying the estimates $\hat{\boldsymbol{\theta}}$ and $\hat{\mathbf{A}}_{1,-},\ldots,\hat{\mathbf{A}}_{K,-}$ in (2).

3 Results and Conclusions

The resulting (trended) heartbeat estimate (black curve in Fig. 1C) highly agrees with a corresponding estimate computed with the algorithm in [2] ($r = 0.999518$).

Compared to the algorithm in [2], the algorithm proposed in this paper is (i) faster, (ii) able to estimate K from the measured signal, (iii) able to estimate the LFO, and (iv) confirmed through many more results from functional studies [4].

References

1. T. Katura, N. Tanaka, A. Obata, H. Sato, and A. Maki, “Quantitative evaluation of interrelations between spontaneous low-frequency oscillations in cerebral hemodynamics and systemic cardiovascular dynamics,” NeuroImage, vol. 31, pp. 1592-1600, 2006.
2. I. Trajkovic, C. Reller, M. Wolf, and H.-A. Loeliger, “A New Approach in Modelling and Filtering Periodic Signals applied to Near Infrared Spectroscopy,” *Proc. 17th European Signal Proc. Conf. (EUSIPCO)*, pp. 632-636, 2009.
3. H.-A. Loeliger, Justin Dauwels, Junli Hu, Sascha Korl, Li Ping and Frank R. Kschischang, ”The factor graph approach to model-based signal processing,” *Proc. of the IEEE,* vol. 95, pp. 1295-1322, 2007.
4. I. Trajkovic, ”Modelling and Filtering Almost Periodic Signals by Time-Varying Fourier Series with Application to Near-Infrared Spectroscopy” Ph.D. thesis, ETH Zurich.

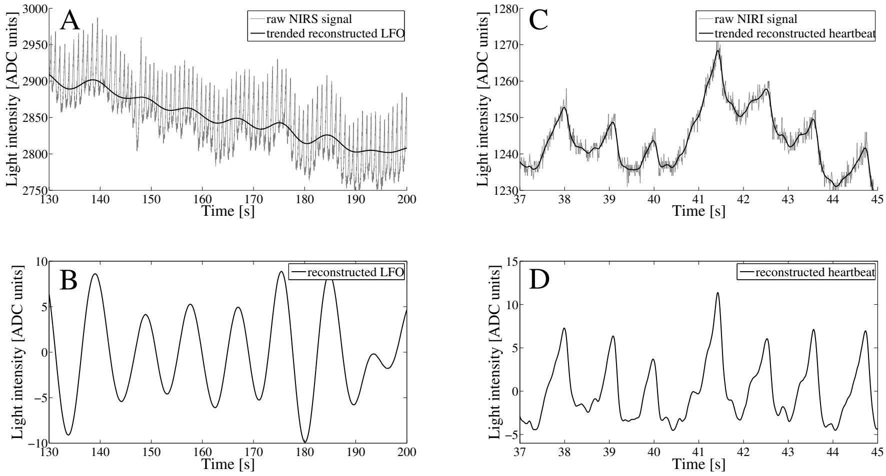

Fig. 1. The grey curves in A and C are raw NIRS signals sampled at 100 Hz. The black curve in C is the reconstructed heartbeat including the estimated slow trend $\hat{\mathbf{A}}_{0,-}$; the black curve in A is the same for the LFO; B is the LFO without $\hat{\mathbf{A}}_{0,-}$; D is the heartbeat without $\hat{\mathbf{A}}_{0,-}$. The heartbeat is also recognisable in A (spikes in the grey curve). The signal values are given in "ADC units" since the NIRS instrumentation uses an Analog-to-Digital Converter (ADC) to digitise light intensity values.

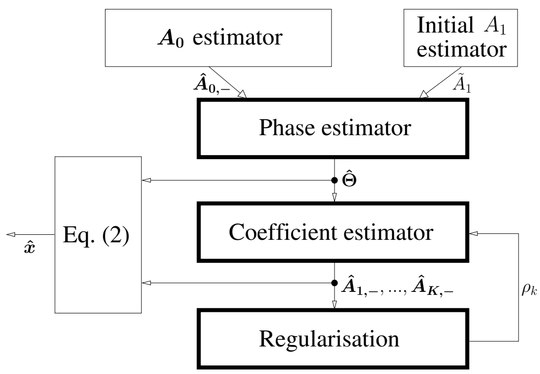

Fig. 2. The building blocks of the proposed algorithm.

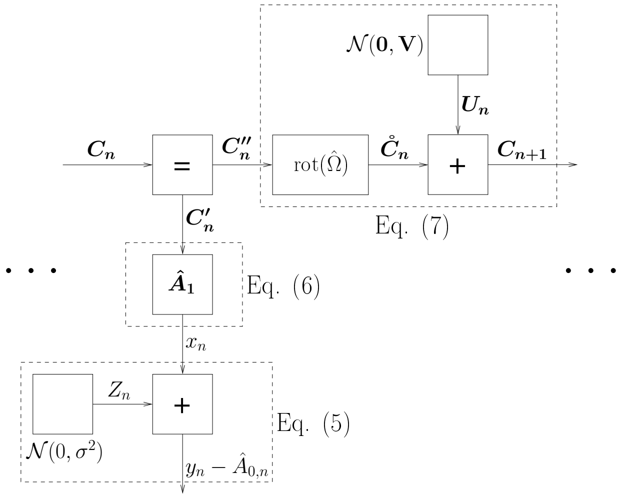

Fig. 3. Factor graph used for estimating $\mathbf{C}_n$.